

## Toward lifetime and $g$ factor measurements of short-lived states in the vicinity of $^{208}\text{Pb}$

This content has been downloaded from IOPscience. Please scroll down to see the full text.

2017 Phys. Scr. 92 054004

(<http://iopscience.iop.org/1402-4896/92/5/054004>)

View [the table of contents for this issue](#), or go to the [journal homepage](#) for more

Download details:

IP Address: 188.184.64.214

This content was downloaded on 30/04/2017 at 19:43

Please note that [terms and conditions apply](#).

You may also be interested in:

[Nuclear-structure studies of exotic nuclei with MINIBALL](#)

P A Butler, J Cederkall and P Reiter

[Measuring the collectivity of neutron-rich nuclei](#)

Andreas G3rgen

[Towards detailed knowledge of atomic nuclei -the past, present and future of nuclear structure investigations at GSI](#)

J Gerl, M Grska and H J Wollersheim

[Coulomb excitation studies of shape coexistence in atomic nuclei](#)

Andreas G3rgen and Wolfram Korten

[Exploring the evolution of the shell structure by means of deep inelastic reactions: recent results from LNL](#)

Giacomo de Angelis

[Inspirations from the theories of Bohr and Mottelson: a Canadian perspective](#)

D Ward, J C Waddington and C E Svensson

[Investigation of exotic nuclei with absolute transition probabilities](#)

A Dewald

[The Legnaro National Laboratories and the SPES facility: nuclear structure and reactions today and tomorrow](#)

Giacomo de Angelis and Gianni Fiorentini

# Toward lifetime and $g$ factor measurements of short-lived states in the vicinity of $^{208}\text{Pb}$

D Ralet<sup>1</sup>, G Georgiev<sup>1</sup>, A E Stuchbery<sup>2</sup>, E Clément<sup>3</sup>, A Lemasson<sup>3</sup>, C Michelagnoli<sup>3</sup>, M Rejmund<sup>3</sup>, L Atanasova<sup>4</sup>, D L Balabanski<sup>5</sup>, G Bocchi<sup>6</sup>, R Carroll<sup>7</sup>, A Dewald<sup>8</sup>, J Dudouet<sup>9</sup>, B Fornal<sup>10</sup>, G de France<sup>3</sup>, S Franchoo<sup>11</sup>, C Fransen<sup>8</sup>, C Müller-Gatermann<sup>8</sup>, A Goasduff<sup>12</sup>, A Gadea<sup>13</sup>, B Jacquot<sup>3</sup>, P R John<sup>14</sup>, D Kocheva<sup>15</sup>, T Konstantinopoulos<sup>1</sup>, A Korichi<sup>1</sup>, A Kusoglu<sup>5,16</sup>, S M Lenzi<sup>14</sup>, S Leoni<sup>6</sup>, J Ljungvall<sup>1</sup>, R Lozeva<sup>17</sup>, A Maj<sup>10</sup>, A Navin<sup>3</sup>, R Perez<sup>13</sup>, N Pietralla<sup>18</sup>, C Shand<sup>7</sup>, O Stezowski<sup>9</sup> and D Yordanov<sup>11</sup>

<sup>1</sup> CSNSM, Univ. Paris-Sud, CNRS/IN2P3, Université Paris-Saclay, F-91405 Orsay, France

<sup>2</sup> Department of Nuclear Physics, Australian National University, Canberra ACT 2601, Australia

<sup>3</sup> GANIL, CEA/DRF-CNRS/IN2P3, Bd. Henri Becquerel, BP 55027, F-14076 Caen, France

<sup>4</sup> Department of Medical Physics and Biophysics, Medical University—Sofia, 1431 Sofia, Bulgaria

<sup>5</sup> ELI-NP, Horia Hulubei National Institute of Physics and Nuclear Engineering, 077125 Magurele, Romania

<sup>6</sup> Istituto Nazionale di Fisica Nucleare, Milano, I-20133 Milano, Italy

<sup>7</sup> Department of Physics, University of Surrey, Guildford GU2 7XH, United Kingdom

<sup>8</sup> Institut für Kernphysik, Universität zu Köln, D-50937 Cologne, Germany

<sup>9</sup> Université de Lyon, Université Lyon-1, CNRS/IN2P3, UMR5822, IPNL, F-69622 Villeurbanne Cedex, France

<sup>10</sup> Institute of Nuclear Physics (IFJ), PAN, 31-342 Krakow, Poland

<sup>11</sup> Institut de Physique Nucléaire, CNRS/IN2P3-Université Paris-Sud, F-91406 Orsay, France

<sup>12</sup> Dipartimento di Fisica and INFN, Sezione di Padova, I-25131 Padova, Italy

<sup>13</sup> Instituto de Física Corpuscular, CSIC-Universidad de Valencia, E-46071 Valencia, Spain

<sup>14</sup> Dipartimento di fisica e Astronomia, Università degli Studi di Padova and INFN, Sezione di Padova, I-35131 Padova, Italy

<sup>15</sup> Faculty of Physics, St. Kliment Ohridski University of Sofia, 1164 Sofia, Bulgaria

<sup>16</sup> Department of Physics Faculty of Science, Istanbul University, Vezneciler/Fatih, 34134, Istanbul, Turkey

<sup>17</sup> IPHC/CNRS-University of Strasbourg, F-67037 Strasbourg, France

<sup>18</sup> Institut für Kernphysik, Technische Universität Darmstadt, D-64289 Darmstadt, Germany

E-mail: [damian.ralet@csnsm.in2p3.fr](mailto:damian.ralet@csnsm.in2p3.fr)

Received 1 March 2017, revised 14 March 2017

Accepted for publication 27 March 2017

Published 20 April 2017



## Abstract

The multi-nucleon transfer reaction mechanism was used to produce and study nuclei in the vicinity of  $^{208}\text{Pb}$ . This mass region is a test case for the nuclear shell model. The mass identification of the fragments was performed with the large acceptance magnetic spectrometer VAMOS++ coupled to the AGATA  $\gamma$ -tracking array. This experiment aimed to determine both lifetimes and gyromagnetic ratios of excited states with the Cologne plunger device. The analysis indicates promising results with the possibility to determine several new lifetimes in this region.

Keywords: multi-nucleon transfer reaction, lifetime measurement, AGATA, VAMOS++

(Some figures may appear in colour only in the online journal)

## 1. Introduction

The structure around doubly magic nuclei is crucial to understanding nuclear effective interactions. The nuclei in the region around  $^{208}\text{Pb}$  allow some specific tests of the nuclear shell model. In particular, there is strong coupling between the octupole vibration of the  $^{208}\text{Pb}$  core and the adjacent high- $j$  orbits. While much is known, the population and identification of many nuclei near  $^{208}\text{Pb}$  is a challenge. For example,  $^{206}\text{Hg}$  with two proton holes in the  $Z = 82$  closed shell, has no reduced transition strength ( $B(E2 : 2^+ \rightarrow 0^+)$ ) measured. The last measured gyromagnetic factor ( $g$  factor) of short-lived state in the mercury isotopic chain is known for  $^{204}\text{Hg}$  [1] with large uncertainties. A  $g$ -factor measurement of low lying excited states of  $^{206}\text{Hg}$  would allow one to deduce the composition of the wave function, and have a direct access to the nature of the excitation.

The work presented here is based on an experiment performed at GANIL to measure lifetimes and  $g$  factors in the vicinity of  $^{208}\text{Pb}$ . The nuclei of interest were produced by multi-nucleon transfer reactions. The experimental setup that allowed us to identify the ejectile and measure the emitted  $\gamma$ -rays will be presented in section 2. The preliminary results obtained are given in section 3.

## 2. Experiment

A  $^{208}\text{Pb}$  beam at 6.25 MeV/A, accelerated by the CSS1 cyclotron, impinging on a  $1 \text{ mg cm}^{-2}$  thick enriched  $^{100}\text{Mo}$  target. The beam-like ejectiles were detected by the large acceptance spectrometer VAMOS++ [2] positioned at the grazing angle of 26 degrees. The  $\gamma$ -rays from reaction fragments were detected in coincidence with the Advanced Gamma Tracking Array [3] (AGATA), positioned at backward angles. In order to maximize the solid angle coverage, AGATA was placed at 148.5 mm from the target, thus 86.5 mm closer than its nominal position. Additional details on the AGATA installation in GANIL can be found in [4].

In VAMOS++, the positions and trajectories of the ions were measured by dual-position sensitive Multi-Wire Proportional Counter [5] (MWPC), positioned at the entrance of the spectrometer, and by a set of four drift chambers (DC), located at the focal plane of the spectrometer. These positions allowed us to reconstruct the trajectories of the ejectiles inside VAMOS++ and to calculate their magnetic rigidity  $B\rho$ . The ions' time-of-flight was measured between the entrance MWPC and the Multi-Wire Parallel Plate Avalanche Counter (MWPPAC) positioned at the VAMOS++ focal plane [2]. The flight path was  $\sim 7.5 \text{ m}$ . The MWPPAC was segmented in 20 independent sections labeled from 0 (low  $B\rho$  value) to 19 (high  $B\rho$  value). The velocity  $\beta$  of the ions was determined by combining the path of the ions with the time of flight. The mass-over-charge ratio ( $M/Q$ ) was calculated by:

$$M/Q = \frac{B\rho}{3.105 \cdot \beta \cdot \gamma}, \quad (1)$$

**Table 1.** Summary of the statistic recorded for each plunger distance. The distance  $\infty$  corresponds to the run without the degrader foil. The difference in the identification efficiency was explained by a change of  $B\rho$  setting for the VAMOS++ spectrometer.

Distances ( $\mu\text{m}$ )	Number of ions at the focal plane identified of mass 207			Number of $\gamma$ -rays $19/2^- \rightarrow 13/2^+$
30	$9.9 \cdot 10^7$	$2.2 \cdot 10^7$	$1.3 \cdot 10^6$	$2.4 \cdot 10^2$
75	$1.3 \cdot 10^8$	$1.0 \cdot 10^8$	$9.4 \cdot 10^6$	$6.1 \cdot 10^2$
200	$1.4 \cdot 10^8$	$4.0 \cdot 10^7$	$3.9 \cdot 10^6$	$9.2 \cdot 10^2$
400	$1.0 \cdot 10^8$	$2.0 \cdot 10^7$	$1.1 \cdot 10^6$	$1.6 \cdot 10^2$
625	$1.3 \cdot 10^8$	$3.5 \cdot 10^7$	$2.4 \cdot 10^6$	$6.8 \cdot 10^2$
1000	$1.4 \cdot 10^8$	$4.1 \cdot 10^7$	$4.0 \cdot 10^6$	$8.0 \cdot 10^2$
2000	$1.2 \cdot 10^8$	$4.7 \cdot 10^7$	$2.7 \cdot 10^6$	$3.8 \cdot 10^2$
4000	$1.4 \cdot 10^8$	$4.6 \cdot 10^7$	$4.4 \cdot 10^6$	$1.0 \cdot 10^3$
$\infty$	$1.1 \cdot 10^8$	$1.8 \cdot 10^7$	$8.0 \cdot 10^5$	$3.9 \cdot 10^1$

with  $\gamma = 1/\sqrt{1 - \beta^2}$ .

The mass of the ejectile was determined by the total kinetic energy of the fragment measured by the ionization chambers (IC) at the focal plane of VAMOS++. The magnetic rigidity of the spectrometer was chosen to increase the flight time of the ions through the spectrometer, thus to select low velocity reaction products. As a consequence, the energies of the ions implanted in the IC corresponded to the Bragg peak, thus were not linearly proportional to the mass of the fragment. Therefore, a velocity-dependant correction factor was applied on the energy measured by the ionization chamber. From this mass estimate, we could calculate the charge state  $Q$  from equation (1). The mass of each fragment was refined by inserting the closest integer value of  $Q$  in equation (1).

The Cologne plunger [6] was installed in the reaction chamber with a  $2 \text{ mg cm}^{-2}$  thick  $^{58}\text{Ni}$  degrader. In addition to a run without degrader foil, data for a total of eight distances from 30 to 4000  $\mu\text{m}$  were recorded. Statistics for each distance are given in table 1. The distances were chosen to cover a large range of lifetimes from 10 to 200 ps. This set of distances provided conditions suitable for a  $g$  factor measurement using the recoil in vacuum method in its time-dependent form (TDRIV); see [7, 8] and references therein.

In order to perform the Doppler correction of the  $\gamma$ -ray energies, the angle between the ejectile and the  $\gamma$ -ray ( $\theta$ ) was calculated using the direction given by the entrance MWPC and the direction of the first  $\gamma$ -ray interaction position given by the Orsay Forward Tracking (OFT) algorithm [9]. The time-of-flight of the ions was measured by averaging the time of the particle passing through the entrance detector (MWPC) and the vacuum space inside VAMOS++. The velocity of the ions at the target position was therefore greater than the one measured inside VAMOS++. A correction factor of 6% was applied to the VAMOS++ velocity to perform the Doppler corrections of the  $\gamma$ -ray energy.

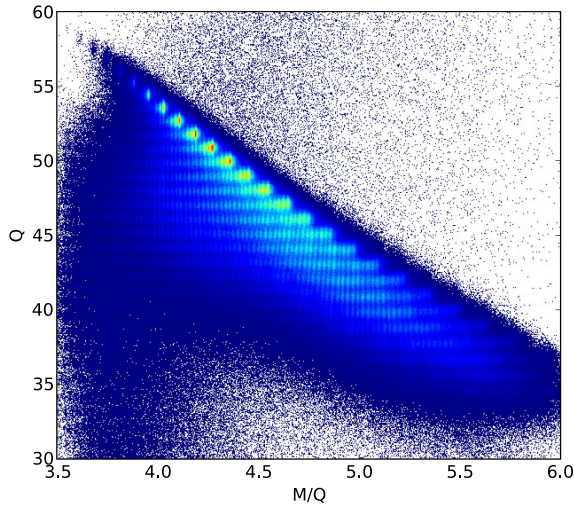


**Figure 1.** Identification of the mass with the VAMOS++ detectors based on the reconstruction of the charge state ( $Q$ ) and the mass over charge ratio ( $M/Q$ ). The matrix was constructed summing the events from MWPPAC number 5 and 6.

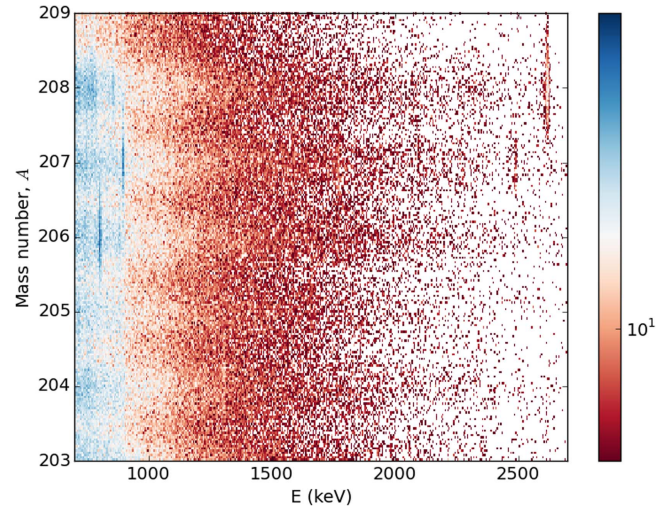


**Figure 2.** Mass of the ejectile as a function of the Doppler corrected  $\gamma$ -ray energy obtained after OFT tracking [9]. This matrix was obtained for the data set without degrader foil.

### 3. Results

The preliminary analysis showed that it was possible to identify the mass and the charge state of the ejectiles with mass  $A \approx 200$  with the VAMOS++ spectrometer. As an example, the number of ions identified with mass 207 is given in table 1. Nevertheless, the determination of the proton number was not possible with the spectrometer. The energy of the x-rays measured with the AGATA detectors is a characteristic of the  $Z$  that can be used to assign the observed  $\gamma$ -ray to the proper nuclei and to determine the presence of an isobaric contaminant in the  $\gamma$ -ray spectra.

A histogram where the charge state  $Q$  is plotted as a function of  $M/Q$  was used to determine the mass of the ejectiles. It is shown in figure 1, and was obtained for the two MWPPAC focal plane detectors (labeled 5 and 6) with the best timing resolution.

The best mass resolution was achieved for the fifth and sixth MWPPAC with a resolution at full width half maximum (FWHM) of  $\Delta M/M = 0.38\%$  and  $\Delta M/M = 0.40\%$  respectively.

The mass identification can also be verified by known  $\gamma$ -ray transitions of the  $^{206,207,208}\text{Pb}$  isotopes, favorably populated in this reaction. For instance, in the matrix of figure 2, the transition from the one-phonon octupole state [10] that decays to the ground state of  $^{208}\text{Pb}$  with an energy of 2614 keV is observed. For mass 207, we clearly observed the 898 keV transition that is assigned [11] to the decay of the  $3/2^-$  state to the ground state of spin  $1/2^-$ . In the mass 206, the  $2^+ \rightarrow 0^+$  transition in  $^{206}\text{Pb}$  was observed with an energy of 803 keV [12].

The  $\gamma$ -ray spectrum shown in figure 3 was obtained with a selection of the mass number 207. In this spectrum, the transitions from the low-spin states decaying to the ground state are clearly identified. The transition with an energy of 2485 keV is the decay of the  $19/2^-$  excited state of  $^{207}\text{Pb}$  built on top of the  $13/2^+$  isomer [13, 14]. This isomer at

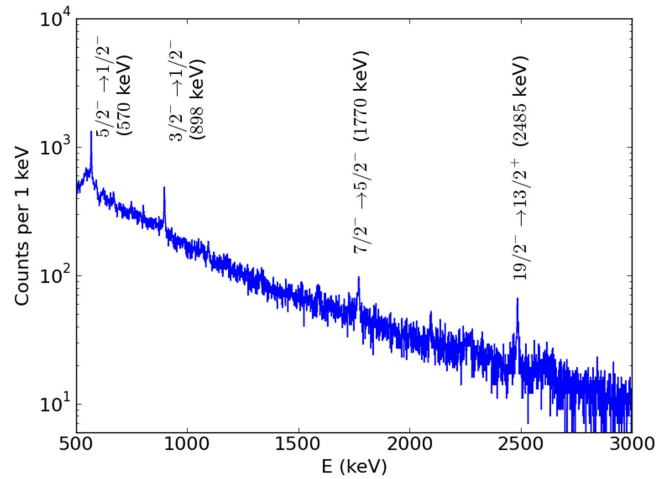


**Figure 3.** Doppler corrected  $\gamma$ -ray spectrum gated on the mass 207. The most populated transitions are indicated on the plot and belongs to  $^{207}\text{Pb}$ . The histogram shown here was obtained for the data without degrader foil.

1633 keV is suggested to be built on the neutron-hole  $\nu i_{13/2}$ . The state at 4119 keV decays to this isomer by a 2485 keV  $\gamma$ -ray transition and has an octupole character [14]. The lifetime measurement of this state would allow us to determine whether it is a two-phonon vibration-coupled state [10] or not. The number of  $\gamma$ -rays recorded for this transition (see table 1) is sufficient to assure the possibility of determining the lifetime of this state, which will be presented in a further publication.

### 4. Conclusion

The results presented here show some of the challenges when studying the region around  $^{208}\text{Pb}$ . With VAMOS++, coupled to AGATA, it was possible to investigate this region with multi-nucleon transfer reactions. The work demonstrated the

power of VAMOS++ to identify ejectiles up to mass  $A \approx 200$ . Further analysis of the data is needed to extract lifetimes of the transitions observed in the experiment. The analysis to date has demonstrated the possibility of determining the lifetime of the  $19/2^-$  state in  $^{207}\text{Pb}$ , which will allow one to determine whether the first excited state above the  $13/2^+$  isomer of  $^{207}\text{Pb}$  has a two octupole-phonon character or not. Additional nuclei were populated in this experiment and the  $g$  factor and lifetime measurements of the transitions observed will be presented elsewhere.

## Acknowledgments

The authors are grateful for the help of the GANIL staff and of the AGATA collaboration. This work was supported by the European Union Seventh Framework through ENSAR (Contract No. 262010). DR was supported by the P2IO

excellence laboratory. This work has also been supported by the Bulgarian NSF Contract No. DFNI-E02/6.

## References

- [1] Kölbl W R *et al* 1986 *Nucl. Phys. A* **448** 123–36
- [2] Rejmund M *et al* 2011 *Nucl. Instrum. Methods A* **646** 184
- [3] Akkoyun S *et al* 2012 *Nucl. Instrum. Methods A* **668** 26
- [4] Clément E *et al* 2017 *Nucl. Instrum. Methods A* **885** 1–12
- [5] Vanderbrouck M *et al* 2016 *Nucl. Instrum. Methods A* **812** 112–7
- [6] Dewald A *et al* 2012 *Prog. Part. Nucl. Phys.* **67** 786
- [7] Stuchbery A E *et al* 2005 *Phys. Rev. C* **71** 047302
- [8] Kusoglu A *et al* 2015 *Phys. Rev. Lett.* **114** 062501
- [9] Lopez-Martens A *et al* 2004 *Nucl. Instrum. Methods A* **533** 454–66
- [10] Hamamoto I 1974 *Phys. Rep.* **10** 63
- [11] Kondev F G *et al* 2011 *Nucl. Data Sheets* **112** 707
- [12] Kondev F G *et al* 2008 *Nucl. Data Sheets* **108** 1527
- [13] Shand C M *et al* 2015 *Acta Phys. Pol. B* **46** 619
- [14] Podolyák Z *et al* 2015 *J. Phys.: Conf. Ser.* **580** 012010